Journal of Theoretical Biology ▮ (▮▮▮▮) ▮▮▮–▮▮▮

Contents lists available at SciVerse ScienceDirect

Journal of Theoretical Biology

journal homepage: www.elsevier.com/locate/yjtbi

A model for *Vibrio cholerae* colonization of the human intestine

Q1 Anna Maria Spagnuolo [a], Victor DiRita [b], Denise Kirschner [b,*]

Q2 [a] Department of Mathematics and Statistics, Oakland University, Rochester, MI 48309-4485, United States
[b] Department of Microbiology and Immunology, 6730 Medical Science II, University of Michigan Medical School, Ann Arbor, MI 48109-0260, United States

ARTICLE INFO

Article history:
Received 16 June 2011
Received in revised form
22 August 2011
Accepted 23 August 2011

Keywords:
Finite element method
Convection
Reaction
Diffusion
Cryptotaxis

ABSTRACT

Vibrio cholerae is a strict human pathogen that causes the disease cholera. It is an old-world pathogen that has re-emerged as a new threat since the early 1990s. *V. cholerae* colonizes the upper, small intestine where it produces a toxin that leads to watery diarrhea, characterizing the disease (Kahn et al., 1988). The dynamics of colonization by the bacteria of the intestines are largely unknown. Although a large initial infectious dose is required for infection, data suggests that only a smaller sub-population colonizes a portion of the small bowel leading to disease. There are many barriers to colonization in the intestines including peristalsis, fluid wash-out, viscosity of the mucus layer, and pH. We are interested in identifying the mechanisms that allow this sub-population of bacteria to survive and colonize the intestines when faced with these barriers. To elaborate the dynamics of *V. cholerae* infection, we have developed a mathematical model based on a convection–diffusion–reaction–swimming equation capturing bacterial dynamics coupled with Stokes equations governing fluid velocity where we developed a novel non-local boundary condition. Our results indicate that both host and bacterial factors contribute to bacterial density in the gut. Host factors include intestinal diffusion and convection rates while bacterial factors include adherence, motility and growth rates. This model can ultimately be used to test therapeutic strategies against *V. cholerae*.

1. Introduction

Diarrheal disease is a leading cause of morbidity and mortality in the world today. *Vibrio cholerae*, the causative agent of cholera, is a key pathogen inducing diarrhea throughout the world. It is ingested through infected water or food products and once it establishes infection, it induces a severe watery diarrhea that persists for days to weeks. This can lead to dehydration and death if not treated. Cholera is most prevalent in the developing world, particularly in warm climates, and *V. cholerae* has been shown to Q4 be seasonally correlated (Rodo et al., 2002).

Upon ingestion, the majority of bacteria are killed by the acidic pH in the stomach. Those that survive enter the lumen of the small intestine and begin colonization. Data suggest that human inoculum size is likely large, since there is approximately a 4–6 log reduction of *V. cholerae* by due to the low pH in the stomach (Cash et al., 1974). A certain percentage of bacteria swim towards the epithelial cells, defying the influence of the convective current (derived from water or digested food), also withstanding propulsive gut mobility (Guentzel et al., 1977).

While near the epithelium, *V. cholerae* makes a potent enterotoxin, cholera toxin, which modifies a key regulatory protein in intestinal cells. The ultimate effect of cholera toxin is constitutive cyclic AMP production in intoxicated cells that results in the opening of normally gated channels in the membrane. This leads to loss of chloride and other ions from the cells, followed by water. The result for the infected individual is massive fluid and ion loss in the form of a watery diarrhea that is the hallmark of cholera infection. The diarrhea in cholera can reach volumes of 20 l per day and leads to shock and death if not treated by oral rehydration therapy (DiRita, 2000). As fluid is introduced into the intestine the bacterial population is subject to the influence of convective flow (Ghorai and Hill, 1999; Kessler, 1986, 1989).

The prevailing assumption regarding dynamics of *V. cholerae* within the intestinal tract is that bacteria close to the epithelium cease to swim and begin to adhere as a necessary step towards colonizing the host. Experiments performed on mice and rabbits reveal that bacteria are found concentrated within the crypts (Schrank and Verwey, 1976; Guentzel et al., 1977), the structure of which may allow for protection against removal by natural intestinal flows. Adherence of bacteria through elaboration of extracellular organelles such as the toxin-coregulated pilus (TCP) is likely to be a key feature of *V. cholerae* pathogenicity (DiRita, 2000). However, the contribution of the adherent population within the context of the larger overall microbial population in an infected

Q3 * Corresponding author.
E-mail addresses: spagnuol@oakland.edu (A. Maria Spagnuolo), vdirita@umich.edu (V. DiRita), kirschne@umich.edu (D. Kirschner).

0022-5193/$ - see front matter © 2011 Elsevier Ltd. All rights reserved.
doi:10.1016/j.jtbi.2011.08.028

intestine is more difficult to assess using experimental models, although recent advances have allowed this adherent population to be more carefully studied (Lee et al., 1999). A series of mathematical models representing bacteria colonization of the human stomach by *Helicobacter pylori* showed that adherence was an integral factor of colonization (Blaser and Kirschner; Blaser and Kirschner, 1995; Joseph and Kirschner, 2004). These models were two-compartmental ordinary differential equations systems representing the relevant spatial aspects of the stomach (lumen, mucous layer, epithelium). The intestines are more complex in space and length, and also have a strong fluid flow present, so different mathematical models are necessary to capture the dynamics of *V. cholerae* in the gut.

While animal models and bacterial genetics have begun to unravel the natural history and pathogenesis for this centuries old pathogen, many aspects of the interaction between *V. cholerae* and its human host remain unknown. For example, while the primary determinants of *V. cholerae* colonization include adhesion, mobility and toxin production (DiRita, 2000) less is known about the dynamics of the interactions of these processes with the human host. Similarly, host factors such as pre-existing immunity and both physical and physiological responses in the gut likely play key roles and may directly or indirectly affect bacterial factors. Animal models allow for some analysis of the host–pathogen interaction in humans. However the ability to study and manipulate groups of variables individually or collectively in these models is currently experimentally limited.

To this end, we have developed a novel mathematical model describing the dynamics of *V. cholerae* in the human intestine. Our overall objective is to gain an understanding of the mechanisms that control the interaction between *V. cholerae* and the human host. Elaboration of processes that allow the microbe to sense and respond to its host environment will allow us to apply the model to explore antimicrobial therapies. These therapies could be aimed, for example, at blocking bacterial mechanisms as well as physical forces acting on the microbe as it establishes itself in the host.

2. Methods

In the course of *V. cholerae* colonization, several processes co-exist: bacterial growth, motility, and diffusion of bacteria and convective fluid flow in the gut from the digestive process and from water excreted from walls of the intestines. The latter process (diarrhea) is triggered by toxic stimulation caused by *V. cholerae*, and is therefore absent during initial colonization events. The life cycle of bacteria evolves from the interaction of these processes, and the goal of this work is to study the dynamics of its evolution. As a first approach, we derive a mathematical model for density of bacteria and velocity of fluid that flows through the intestinal cross-section.

Developing a model to study *V. cholerae* dynamics in the human intestines requires us to consider factors related to both bacteria and host. Bacterial factors constitute sub-populations of invading bacteria and their different functional characteristics, while host factors include structural and physiological environmental factors that impact *V. cholerae*. We describe these in detail together with the derivation of the mathematical model representing this system.

2.1. Modeling the bacteria

As noted in animal experiments, most notably in the infant rabbit model, which most closely replicates human pathogenesis, bacteria are found adherent throughout the epithelial surface including within crypt-like structures (Ritchie et al., 2010). Data from sensitive measures of gene expression during infection of mice show that only a small fraction of the initial inoculum reaches the appropriate micro-environment of the intestine that allows for colonization (Lee et al., 1999), suggesting that this sub-population is critical for establishing infection. In other words, the majority of the inoculum, which do not express factors for adherence, likely do not contribute to the infection. This is a similar observation to that shown in models of *H. pylori* where the adherent population serves as an epidemic 'core' population driving infection dynamics (Blaser and Kirschner; Blaser and Kirschner, 1995; Joseph and Kirschner, 2004).

Based on these considerations, we define three mutually exclusive sub-populations of bacteria, namely luminal, mucosal, and epithelium (adherent) populations. As a first assumption, the luminal and mucosal are the motile populations; the environments they reside in directly affect their motility, respectively. For example, the luminal population does not have to contend with the viscosity of the mucus layer. We assume that the adherent population is not motile. Our model also allows for variations in bacterial diffusion (Crank, 1975) in different sub-populations as well as different growth rates in each sub-population (Cooper, 1997). It is reasonable to neglect a term representing bacterial death since it is more likely that bacteria are removed by other mechanisms, such as epithelial cell sloughing in the time period of interest (as in Blaser and Kirschner; Blaser and Kirschner, 1995; Joseph and Kirschner, 2004).

The exact percentage of bacteria that swim *in vivo* is unknown, but is included in the list of model parameters. A strength of modeling is that we can vary the parameters in the model in order to study the dynamics more carefully. For example, we can compare simulated outcomes under different sets of parameter values. This approach could be useful in predicting and understanding *V. cholerae* infection dynamics in humans.

2.2. Modeling the environment

The geometry and composition of a typical cross-section of human intestine is shown in Fig. 1a for readers who are not familiar with villi and crypts. The lumen, mucus layer, and epithelium constitute the basic structure of the intestine. The lumen is the inner cavity, and it allows for the passage of digested food. The mucus layer lies over the epithelium and consists of a gel-like substance that protects the body from bacterial penetration. The epithelium, the surface of the intestinal wall, is composed of epithelial cells which are organized into villi and crypts.

In order to model the dynamics of interest, we define a three-dimensional coordinate system. The standard Cartesian coordinate system consists of three mutually perpendicular directions, namely x_1, x_2, and x_3. However, since the intestinal cross-section is cylindrical, we transform the coordinate system into one involving cylindrical coordinates for convenience. See Fig. 1b for an illustration of the radial, angular, and intestinal length directions, namely r,θ, and z, respectively. Fig. 2 shows a two-dimensional simulation platform for the reduced mathematical model. In a straightforward manner, we use the following conversion formulas (Acheson, 1990)

$$x_1 = r\cos\theta, \quad x_2 = r\sin\theta, \quad x_3 = z,$$

and the orthogonal curvilinear basis $\{e_r, e_\theta, e_z\}$ via the relation

$$e_r = (\cos\theta)e_1 + (\sin\theta)e_2 \tag{1}$$

$$e_\theta = -(\sin\theta)e_1 + (\cos\theta)e_2 \tag{2}$$

$$e_z = e_3 \tag{3}$$

Please cite this article as: Maria Spagnuolo, A., et al., A model for *Vibrio cholerae* colonization of the human intestine. J. Theor. Biol. (2011), doi:10.1016/j.jtbi.2011.08.028

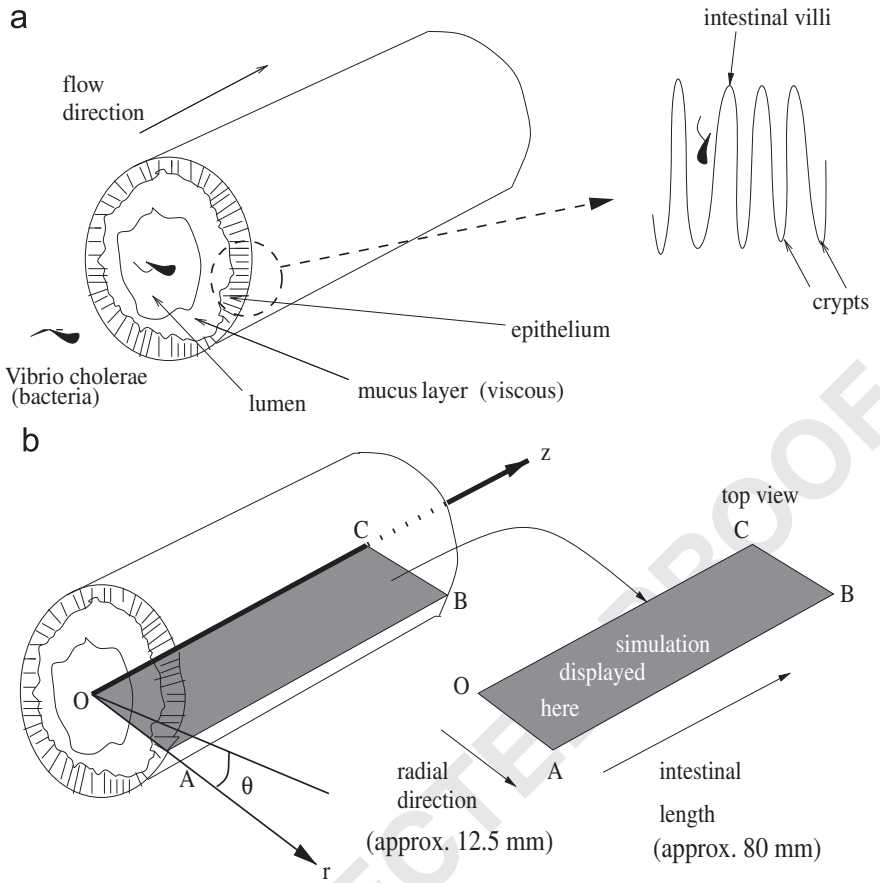

Fig. 1. (a) Small intestinal section. A three-dimensional cross-section of the intestine including the detailed structure of the epithelium, which is composed of villi and crypts. (b) Mathematical framework. The mathematical description of the intestinal cross-section in terms of the coordinates r,z, and θ. The left is the three-dimensional illustration of an intestinal cross section. The rectangular slice OABC is the *display platform* for our simulations (see Fig. 2). The line segment OC represents the line through the center of the lumen, and AB represents the outer edge of the intestinal wall. The three-dimensional result is visualized using radial symmetry of the intestinal section. See http://en.wikipedia.org/wiki/Small_intestine.

where $\{x_k; k=1,2,3\}$ is the Cartesian coordinates and $\{e_k; k=1,2,3\}$ is the standard orthonormal basis in R^3 respectively.

Let v denote the velocity of the water in the intestines. By Eqs. (1)–(3), the cylindrical components of the velocity are given by

$$v_r = v \cdot e_r, \quad v_\theta = v \cdot e_\theta, \quad v_z = v \cdot e_z, \tag{4}$$

where v_r, v_θ, and v_z denote the components along the radial, angular, and tubular directions, respectively. The primary assumptions we make in deriving the mathematical model are stated as follows:

A1: The density of bacteria and the velocity of the water are independent of the angular direction θ.
A2: The angular component of the water velocity, v_θ, is equal to zero.

The assumptions are based on reasonable approximations of the physical quantities with respect to the angle θ, because the flow velocity in the tubular, z, and radial, r, directions are dominant, and the diffusion along different angular directions is similar.

The geometry of the intestinal cross-section (Fig. 1b) is now reduced to a rectangular planar geometry in terms of the cylindrical coordinate directions r and z (Fig. 2). We point out that the topology of the true intestinal region is not changed by our assumptions.

2.3. The fluid flow model

The simulations presented in this work are performed under an assumed velocity profile. However, to keep the model general for future considerations, we derive the equations that govern the water flow through the intestines using standard three-dimensional incompressible non-steady Stokes equations (Foias et al., 2001) for the velocity, since we are assuming a low Reynolds number system (Happel and Brenner, 1987). Recall that v_r, v_θ, and v_z are the radial, angular, and tubular velocity components, respectively. Then, the cylindrical setting as we described above allows us to arrive at the following modified and simplified version of the Stokes equations in the two-dimensional setting:

$$\frac{\partial v_r}{\partial t} = -\frac{1}{\rho}\frac{\partial p}{\partial r} + \mu\left(\Delta v_r - \frac{v_r}{r^2}\right) + F_1, \tag{5}$$

$$\frac{\partial v_z}{\partial t} = -\frac{1}{\rho}\frac{\partial p}{\partial z} + \mu\Delta v_z + F_2, \tag{6}$$

$$\frac{1}{r}\frac{\partial}{\partial r}(rv_r) + \frac{\partial v_z}{\partial z} = 0, \tag{7}$$

where t is the time, μ and ρ are the viscosity and the density of the water, respectively, F_1 and F_2 are external forces, Δ is the θ-independent cylindrical coordinate version of the Laplacian given by

$$\Delta = \frac{1}{r}\frac{\partial}{\partial r}\left(r\frac{\partial}{\partial r}\right) + \frac{\partial^2}{\partial z^2}, \tag{8}$$

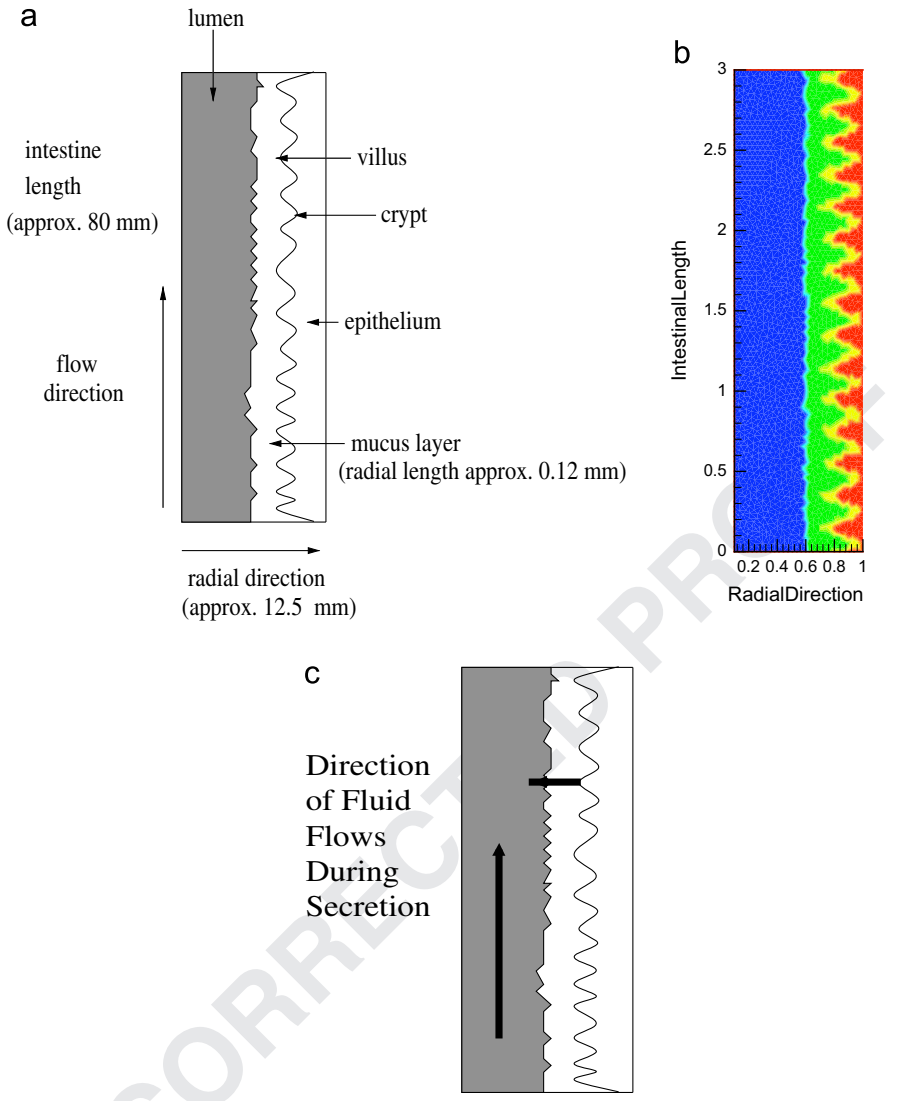

Fig. 2. (a) Simulation display platform (not to scale). A cross-section of the small intestine in two-dimensions. This illustration corresponds to the simulation display platform as indicated in Fig. 1(b) http://en.wikipedia.org/wiki/Small_intestine, http://chestofbooks.com/health/disease/Intestines/Structure-Of-The-Small-Intestine.html. (b) Simulation display with color. The two-dimensional figure shows the computational region used in the simulations. The lumen is the region shown in blue, the mucus is the region shown in yellow, and the epithelium (as a layer) is the region shown in red. The boundary curve separating the mucus from the epithelium is given by $0.9+0.1\sin(10\pi z)$. (c) Fluid flow directions are shown during fluid secretion times. Fluid flows downstream the small intestine due to digestion and fluid flows out of the intestinal wall due to fluid secretion. (For interpretation of the references to color in this figure legend, the reader is referred to the web version of this article.)

and in what follows $v\cdot\nabla$ is understood to be in terms of cylindrical coordinates via

$$v\cdot\nabla = v_r\frac{\partial}{\partial r}+\frac{v_\theta}{r}\frac{\partial}{\partial\theta}+v_z\frac{\partial}{\partial z}. \tag{9}$$

2.4. Derivation of a model for bacterial density

We remark that Eqs. (5)–(9) are the basic equations that describe the flow in the intestinal cross-section, to be coupled with a mass-balance equation for bacteria that we now describe.

Let $u=u(r,\theta,z)$ denote the density of the bacteria in the intestine. Let V be a fixed representative sample volume inside the intestine (Fig. 1b). Denote the boundary of V by ∂V. Then, conservation of mass yields that the rate of change in mass over V is given by

$$\underbrace{\int_V \frac{\partial u}{\partial t}\,dx}_{\text{Total Rate of Change}} = \underbrace{-\int_{\partial V} q\cdot n\,dS}_{\text{Amount Crossing Boundary}} + \underbrace{\int_V cu\,dx}_{\text{Multiplication Change}} + \underbrace{\int_V S\,dx}_{\text{External Influences}}, \tag{10}$$

where q is the flux, c is the coefficient of the reaction term: the birth rate of the bacteria when $c>0$ and the mortality rate when $c<0$; and the last integral in (10) allows for changes in bacterial density due to external sources/sinks S, such as ingestion of bacteria or introduction of antibiotics.

One of the most challenging and important aspects of the mathematical problem involves designing a way to incorporate the necessary components of the flux into the model. We decompose the flux into its diffusion, convection, and motility terms as follows:

$$\text{Flux} = \underbrace{\int_{\partial V} q\cdot n\,dS}_{\text{Amount Crossing Boundary}} = \underbrace{-\int_{\partial V} a\nabla u\cdot n\,dS}_{\text{Diffusion}} + \underbrace{\int_{\partial V} uv\cdot n\,dS}_{\text{Convection}} + \underbrace{k\int_{\partial V}\alpha u e_r\cdot n\,dS}_{\text{Motility}}, \tag{11}$$

where the symmetric diffusion tensor a assumes different values in the lumen, mucus, and epithelium. For this study, it is reasonable to assume that a is a scalar function of radial and length directions only, such that $a=a(r,z)$, since there are no fixed obstructions in the intestine that could define a preferred diffusion direction. The

values of $a(r,z)$ have significant jumps across neighboring layers of the intestinal cross-section, reflecting distinctly different compositions within the intestine. Indeed, the mucus layer is composed of a very viscous gel-like substance which serves as the only barrier against bacterial penetration into the epithelium. Thus the value of $a(r,z)$ is smallest in the mucus layer. However, once bacteria break through the mucus layer they are free to access the epithelium, where they adhere. Thus, the value of $a(r,z)$ is also small in the epithelium. The second integral on the right-hand side of (11) is the standard convection term by which the equation is coupled to the water-flow equations (5)–(9). The motility phenomenon of the bacteria is given by the last integral in (11). This term is absent from the constitutive relations commonly seen in general reaction–diffusion processes (Douglas and Spagnuolo, 2001, 2002; Douglas et al., 2002).

Since experimental data reveal that a percentage k of bacteria swim against the current (likely via chemotaxis) toward the epithelial cells (located in the direction e_r), the motility term resembles a bacterial-initiated convection along a preferred direction (vs. the media-initiated convection). In the motility term, α represents the known swimming velocity of the bacteria in each layer. We turn our attention to the parameter k, an important part of the motility effect. First, $k \in [0,1]$ since not all bacteria swim toward the epithelium. Secondly, its value is set to zero in the epithelium layer reflecting that the bacteria adhere to the epithelium. Physical factors such as peristalsis, epithelial cell sloughing, and diarrhea are the only ways in which they can be removed by the body.

Pointwise versions of Eqs. (10) and (11) are obtained by applications of the divergence theorem, followed by letting $|V| \to 0$. After combining the resulting equations with an appropriate rearrangement of terms, we arrive at an equation in Cartesian coordinates that describes the combined diffusion–convection–motility–reaction process of bacterial density:

$$\frac{\partial u}{\partial t} - \mathrm{div}\{a\nabla u\} + \mathrm{div}\{uv\} + k\alpha\ \mathrm{div}\{ue_r\} - cu = S. \tag{12}$$

Let $\partial\Omega_L$ be the boundary between the epithelium and the mucus and let $J=[0,T]$ be the time interval of interest. We assume that $\alpha = 0$, on $\partial\Omega_L \times J$, since the bacteria do not swim once they reach $\partial\Omega_L$. Since the bacteria adhere to the epithelium, we impose the following boundary conditions on $\partial\Omega_L$:

$$\nabla u \cdot n = 0 \quad \text{on } \partial\Omega_L \times J,$$

$$v \cdot n = -\gamma(u) \quad \text{on } \partial\Omega_L \times J,$$

where $\gamma(u)$ is, in general, a non-decreasing function of the bacterial density. For the purposes of this work, we shall make the following assumption: once the bacterial density reaches a given value of u^* at time t^* on the epithelium, then the body secretes fluids (water and electrolytes, etc.) at a rate of v_{sec} for a duration of T^* days (where $T^* = 3$). That is,

$$\gamma(u) = \begin{cases} 0 & \text{if } 0 \le u \le u^*, \\ v_{sec} & \text{if } u^* < u \text{ for } t \in [t^*, t^*+T^*]. \end{cases}$$

See Fig. 2c for an illustration of fluid flow directions during secretion of fluids.

For example, if we assume the average size of the bacteria is 1 μm long with a radius of 0.25 μm, the maximum possible concentration is $u^* = (16 \times 10^9)/\pi^2$ bacteria/mm^3. The value of v_{sec} that we will take is 6 L/day over the entire epithelial surface in the duodenum.

Let $L = \int_{\partial\Omega_L} v \cdot n\, dS$ be the total velocity of the water that leaves $\partial\Omega_L$ times the surface area of $\partial\Omega_L$. We also impose the following radial symmetry conditions: $(\partial/\partial r)v_r(0,z) = 0$ and $(\partial/\partial r)u(0,z) = 0$.

In addition, we impose no diffusion on the lateral surfaces:

$$\nabla u \cdot n = 0 \quad \text{on } \partial\Omega_{in} \cup \partial\Omega_{out} \times J, \tag{13}$$

and we assume a known initial concentration of inoculum, namely

$$u(x,y,z,0) = u_{init} \quad \text{in } \Omega.$$

We begin by taking a given (parabolic profile) velocity field. With m denoting a given metabolic rate, we define

$$f(r) = \frac{2m}{\pi R^4}(R^2 - r^2), \tag{14}$$

and write $v = (0, f(r))$. Note that $\nabla \cdot v = 0$. In addition, we impose the following boundary conditions on $\partial\Omega_{in}$ and on $\partial\Omega_{out}$:

$$v \cdot \mathbf{n} = -f(r), \quad v_r = 0 \ \text{ on } \partial\Omega_{in} \times J, \tag{15}$$

$$v \cdot \mathbf{n} = f(r) - \frac{L}{\pi R^2}, \quad v_r = 0 \ \text{ on } \partial\Omega_{out} \times J. \tag{16}$$

Next, we transform (12) into cylindrical coordinates using the notation shown at the beginning of this section, and we arrive at the θ-independent cylindrical-coordinate version of conservation of mass in Ω, where Ω is the intestinal cross- section under study:

$$\frac{\partial u}{\partial t} - \left(\frac{1}{r}\frac{\partial}{\partial r}\left(ra(r,z)\frac{\partial u}{\partial r}\right) + \frac{\partial}{\partial z}\left(a(r,z)\frac{\partial u}{\partial z}\right)\right) + \nabla_{r,z} u \cdot v + k\alpha\left(\frac{\partial u}{\partial r} + \frac{1}{r}u\right) - cu = S. \tag{17}$$

This is the desired governing equation for bacterial density. See Appendix A for the derivation of the weak formulation of the model used in the continuous finite element numerical scheme and for the proof of a conservation relation.

2.5. Numerical assumptions and domain specifications

For the simulations presented here, a piecewise linear continuous finite element method was implemented to compute the solution to the bacterial density equation (17). To make the computations straightforward, we assume that the epithelium is a region, rather than a boundary, better reflecting the biology. The model system together with parameter values given in Table 1 were coded in gfortran (GNU Fortran) and were solved on a computer running Cent OS with a 64-bit Intel Xeon Westmere processor and 6 GB of memory.

Table 1
Baseline parameters.

Symbol	Parameters	Simulation value	Reference
α	*V. cholerae* motile velocity	75 μm/s	Atsumi et al. (1996)
k	Fraction of motile bacteria	1	See text
c	Growth rate (doubling time) in lumen and mucus	71 min	Spira and Sack (1982)
v	Convection coefficient (m) for $0 \le r \le 0.8$	0.167 mm/s	Wallace Hayes, 2008, Eq. (14)
A_L	Scaled diffusion coefficient in lumen region	E0.001 mm^2/s	See text
A_M	Scaled diffusion coefficient in mucus region	E0.0001 mm^2/s	See text
A_E	Diffusion coefficient in epithelium region	0 mm^2/s	See text

Please cite this article as: Maria Spagnuolo, A., et al., A model for *Vibrio cholerae* colonization of the human intestine. J. Theor. Biol. (2011), doi:10.1016/j.jtbi.2011.08.028

Our computational domain consists of the region of intestine shown in Fig. 2b. Our finite element mesh was created using the open-source mesh generator, triangle (Shewchuk), which was used to create Delaunay triangles with a maximum area of 0.00025 mm^2. We also used a time step of 0.00025 s. In all simulations, we introduce bacteria in a spherical bolus located in the lumen of the small intestine (see Fig. 3 and the Host and Initial Conditions Subsection for the exact form of the source term S).

As shown in Fig. 1, the small intestinal section is almost one order of magnitude larger, in each of the radial and length directions, than the sizes we are using for our simulations (see Fig. 2b). This is due to the limitations we experienced with computer power and we explore this scaling issue further in the Discussion Section. Because the simulation region is so small, we can capture the dominant colonization dynamics in approximately 15 s for the bacteria in that region. These alterations in the domain specifications are not unreasonable for studying dynamics near the mucus and epithelium. In the current work, we are developing a simulation method based on a locally conservative discontinuous Galerkin Method (Cockburn and Shu, 1998; Cockburn et al., 2000; Arnold et al., 2002; Hesthaven and Warburton, 2008) to capture more biologically realistic space and time scales.

2.6. Parameter estimation

Here we indicate how we estimated values for the majority of the parameters in the model to use for our baseline (standard) case study. Others are studied through numerical simulations of the system in order to calibrate the model and also test for effects. A summary of the parameters and their values is given in Table 1 with references when available.

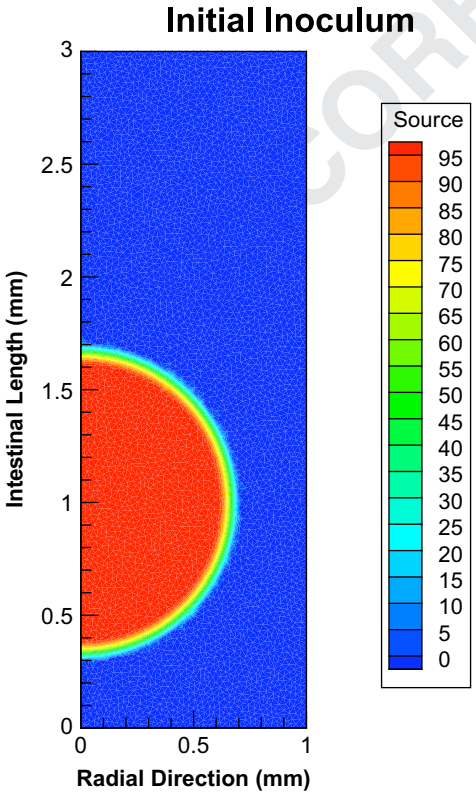

Fig. 3. Bacterial inoculum distribution, measured in the units of number of bacteria per mm^3 per second. In the simulations to follow, it is distributed over a time period of 10 s, after which the value is set to zero.

Based on experiments in which human volunteers were given doses of *V. cholerae* with and without bicarbonate to buffer the stomach acid, then followed for cholera symptoms, there is approximately a 4–6 log reduction of *V. cholerae* due to the low pH environment in the stomach (Cash et al., 1974). Therefore, the number of *V. cholerae* ingested is likely orders of magnitude larger than the number that eventually enters the small intestine. We chose to study colonization dynamics under the assumption that approximately 1000 bacteria enter the lumen of the small intestine (see Fig. 3). Our model is flexible to variations in this number.

Peristalsis rates in the intestine are given in Wallace Hayes (2008). Specifically, the movement of chyme in the small intestine is at a rate of approximately 1 cm/min. Therefore, we use the value $m = 0.167$ mm/s and $R = 0.8$ mm in Eq. (14) for $0 \le r \le 0.8$ for the convection rate $v = (0, f(r))$ throughout our simulation domain shown in Fig. 2b. Also, since *V. cholerae* swims at rates reaching 75 μm/s in media of medium viscosity (Shigematsu et al., 1995), we use this value for the swimming rate in the lumen and in the mucus (up to a distance of 0.05 mm away from the epithelium layer where it is set to 0 for numerical convenience) in our baseline simulations.

Next, studies have shown that increasing viscosity 10-fold reduces maximum swimming rates of a similar bacterium '*V. alginolyticus*' by about two-fold (to approximately 30 μm/s) (Atsumi et al., 1996). In our simulations, we represent this by assuming the diffusion coefficient, A_L, in the lumen is 10 times larger than the diffusion coefficient, A_M, in the mucus. Since there is currently no data on the diffusion values in the lumen and mucus of the small intestine, we chose the following numerically convenient values: $A_L = 0.001$ mm^2/s, $A_M = 0.0001$ mm^2/s, and $A_E = 0$ mm^2/s in the epithelial layer, because bacteria do not cross the epithelial cell layer.

Since the fraction of bacteria that can swim is not known, in our baseline simulations we chose $k = 1.0$, assuming all bacteria swim at the same rate. This will be studied in more detail in future work.

A kinetic analysis using a rabbit model of *V. cholerae* colonization (Spira and Sack, 1982) demonstrated a doubling time of 71 min for *V. cholerae in vivo* for the first 6 h of infection. Therefore, we set $c = 0.00016$ per second in Eq. (17).

2.7. Host and bacterial initial conditions

The initial conditions for the model reflect a healthy host system with the introduction of a single bolus inoculum of bacteria equal to 100 bacteria per mm^3 per second for 10 s. This leads to approximately 1000 bacteria entering the spherical region. While the bacteria are typically ingested and enter the intestines in a non-homogeneous fashion, here we assume that the bacteria enter at the site as a sphere in the 3-D lumen of the intestine (Fig. 1). This is visualized as a semicircular shape in the 2-D representation and is shown in Fig. 3, where the source term is prescribed as

$$S(r,z,t) = \chi_{0 \le t \le 10}(100\chi_{0 \le r \le 0.6} + 100\cos(2(d_0 - 0.6)\pi/0.2)\chi_{0.6 \le r \le 0.7}),$$

where $d_0 = \sqrt{r^2 + (z-1)^2}$, and r and z are measured in millimeters and seconds, respectively. The model is flexible and can test a range of initial inoculum shapes and sizes.

2.8. Simulating infection dynamics of V. cholerae

To begin to study the dynamics of *V. cholerae* infection, we simulated the bacterial density mathematical model (see Section 2.4). The geometry of the region under study is shown in Fig. 1. For clarity of visualization, we demonstrate our simulation results

in a two-dimensional platform. Fig. 2b depicts how the figures that show the simulation results should be interpreted. Our outcome variable of interest is bacterial density. In future work we can also explore other outcome variables.

In the absence of bacteria, the negative control simulations show the system has fluid flow representing a healthy intestine. When bacteria are input into the model, as described in Section 2.7, and it is simulated with parameter values from Table 1, the results of a typical simulation of colonization inside the intestinal region are shown in Fig. 4. We refer to this as our baseline case, at six time points. *Tecplot* was used to create all simulation pictures. As the system evolves in time, bacteria move from the lumen toward the epithelial cells and then colonize.

Note that due to convection, the bacteria cannot migrate directly to the epithelial cells, but they are forced downstream while they attempt to reach the epithelial cells. Bacterial adherence to epithelial cells is evidenced by the high density of bacteria near the epithelial cells. Bacteria have difficulty sustaining a position in the mucus layer due to its gel-like composition (parameterized by a small diffusion coefficient), but once they pass through it, they can colonize at the epithelial cell surface. In the lumen they are washing out as indicated by the lower density values there.

To study the dynamics of our system, we can now alter bacterial factors such as motility and host factors such as convection rates to observe the effects on bacterial colonization.

2.8.1. *Cryptotaxis: a key mechanism of colonization*

Although it has not been explicitly shown experimentally, the behavior of *V. cholerae* is assumed to have the following dynamics: most of the bacteria are motile, a small population migrate through the mucus gel toward the epithelial layer, linking sensing nutrient rich cells. It is here where they are in the close vicinity of intestinal crypts and thus they begin multiplying and producing toxins. Because of the strong convective forces and difficulty penetrating the mucus gel, likely only a small percentage arrive at the epithelial layer. Bacteria then change phenotype from motile to non-motile, adherent. Our model development to this point has assumed this same dynamic.

We define this bacterial-sensored migration along with the self-controlled habitation as *cryptotaxis*. In an experimental

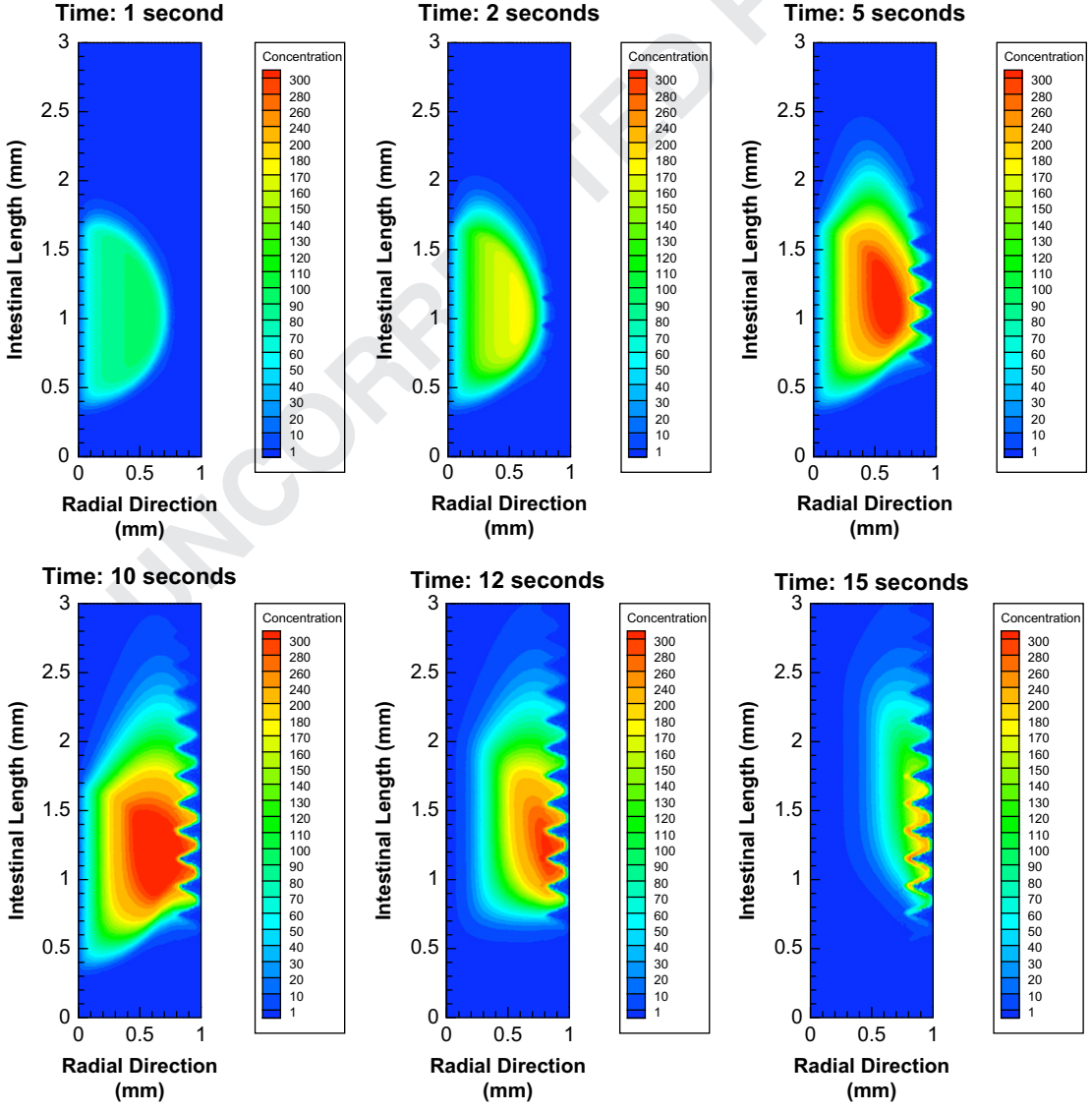

Fig. 4. This is a typical infection scenario we refer to as the virtual wild-type. Shown are changes over time, with time points: 1 s, 2 s, 5 s, 10 s, 12 s, 15 s. Note that the bacteria have difficulty maintaining their position in the mucus layer due to its gel-like composition, but once they pass through it, they colonize the epithelium. Bacteria travel downstream (due to convection).

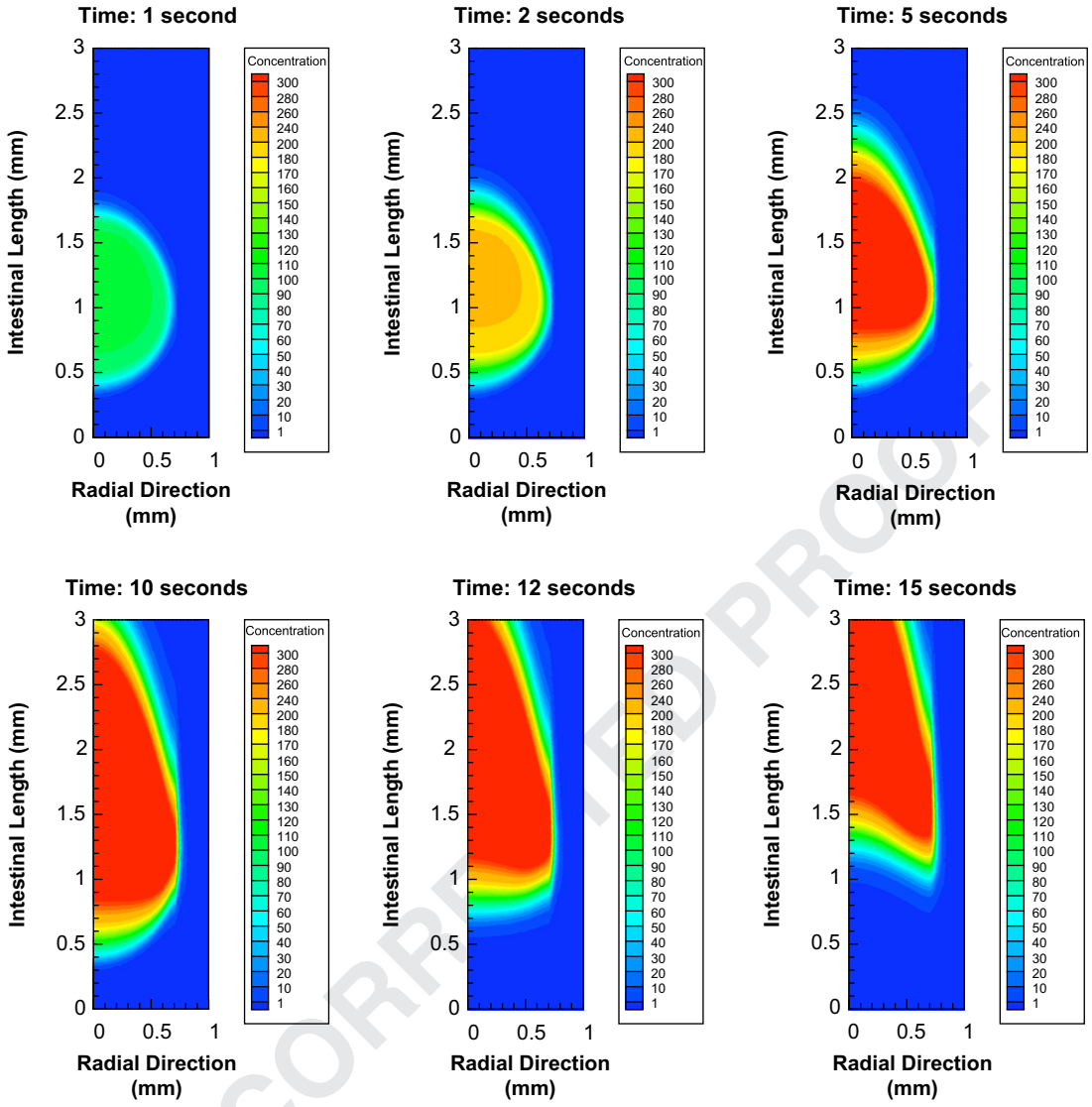

Fig. 5. Virtual knockout of motility. To achieve a virtual simulated motility knockout, the motility parameter is set to zero, while all other parameters are set to the wild-type values (Table 1). The result is dramatically different from wild-type (compare with Fig. 4). Bacterial density pattern is influenced by downstream convection. The washout effect begins to emerge as dominant in comparison to wild-type as the maximum bacterial density decreased one order of magnitude in the knockout simulation. Time points: 1 s, 2 s, 5 s, 10 s, 12 s, 15 s. The bacteria cannot penetrate the mucus layer to colonize before being washed out.

setting it is difficult to quantify cryptotaxis. To test whether *V. cholerae* can colonize in the absence of directed motility, we can compare model simulations where we virtually 'knock-out' the bacteria's ability to swim.

Fig. 5 shows the time-series bacterial dynamics for the simulated directed motile knockout. Comparing that with Fig. 4, it is clear that cryptotaxis is a key mechanism for *V. cholerae* to achieve a colonization.

2.8.2. *Motility in altered convective environment*

It is interesting to study how the environment of the intestines also affects colonization dynamics. In the final simulation, we study the scenario where all parameters are set to their baseline values (Table 1), except that the convection rate of chyme or fluid moving through the intestine, m, is decreased by 50%. This could help us understand how the fluid flow itself affects colonization. Fig. 6 shows the simulation results. One noticeable difference in this case when compared to the wild-type simulation is that bacteria colonize almost directly across (in the radial direction) from the source of the initial inoculation, rather than pushed away from the strong convective force.

3. Discussion

In this work we present the first model capturing the dynamics of *V. cholerae* in the human small intestine. Our goal was to determine which host and bacterial factors contribute to colonization leading to infection versus clearance. Although we did not perform a complete sensitivity analysis of the parameter space in this initial work, we were able to predict some key factors that we will explore in future work.

First, our model suggests that motility, directed by taxis to the crypts, is a key component of colonization of the epithelial layer because the mucus layer presents a challenge to diffusion-based epithelial colonization. From experiments in animal models, the role of chemotaxis and bacterial motility in the pathogenesis of infection by *V. cholerae* has been the subject of investigation, although there remain questions that might be settled with future

Please cite this article as: Maria Spagnuolo, A., et al., A model for *Vibrio cholerae* colonization of the human intestine. J. Theor. Biol. (2011), doi:10.1016/j.jtbi.2011.08.028

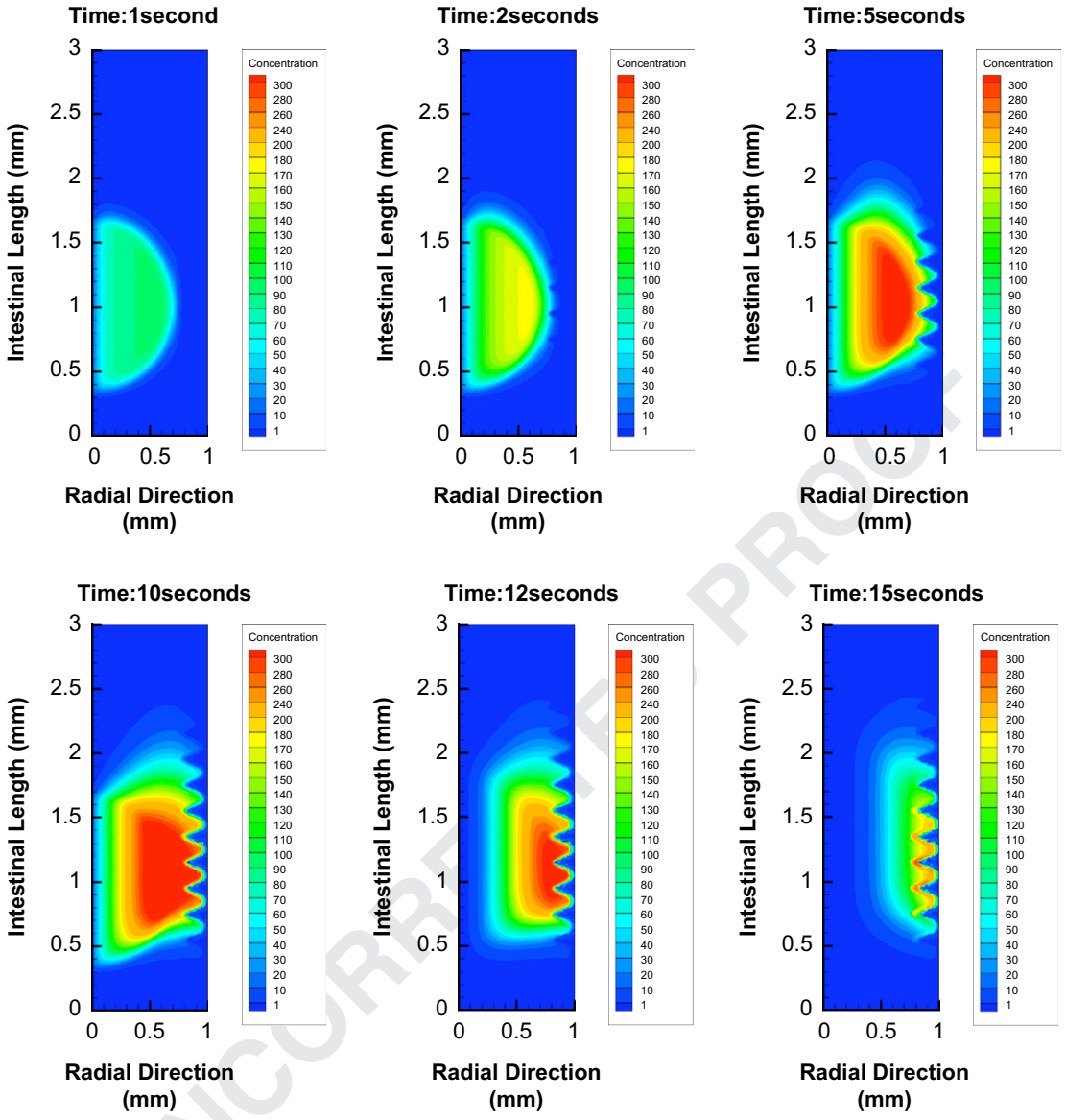

Fig. 6. Low convection significantly enhances colonization. In the current simulation, we decreased the convection rate m by 50% and left all other parameters at their baseline values. Notice that the bacteria colonize closer to the initial inoculation as compared to the baseline case. Also, notice the larger bacterial concentration in the epithelium as compared to the baseline case over the same time points: 1 s, 2 s, 5 s, 10 s, 12 s, 15 s. The low convection allows bacterial motility to dominate so that the bacteria can colonize the epithelium sooner.

mathematical modeling. A strain lacking the major flagellin subunit FlaA was severely attenuated for colonization in competitive assays with wild type bacteria in an infant mouse model (Lee et al., 2001). Chemotaxis directed movement towards or away from attractants or repellants is evidently critical for establishing wild type levels of colonization (Lee et al., 2001; Freter et al., 1981). *V. cholerae* that are rendered genetically unable to respond to stimuli by alternating between smooth swimming and tumbling required for chemotactic behavior, heavily out-compete wild type bacteria in an infant mouse model. However, the colonization behavior is altered and they do not exhibit the same spatial distribution of wild type bacteria within the intestines and their ability to properly regulate virulence gene expression is altered as well (Butler and Camilli, 2004).

Notwithstanding the apparent role for chemotactic-directed motility in the mouse model suggested by the observations noted above, a recent study using an infant rabbit model demonstrated crypt colonization by *V. cholerae* non-motile mutants lacking the major flagellar subunits (Rui et al., 2010). Strains used in this study lack the cholera toxin genes and therefore do not induce the physiological responses of wild type strains in these animals, such as elevated mucin production and secretory diarrhea. The lack of such responses may enable non-motile mutants to colonize crypts more readily than they would in the presence of the secretory response caused by toxins. Another possibility is that chemotactic motility through a flagellar-independent mechanism may direct crypt colonization, a hypothesis supported by the fact that, unlike other motile bacteria, *V. cholerae* encodes multiple sets of chemosensory systems related to motility (Boin et al., 2004).

In addition to host factors, we also explored a host environmental factor and its role in modulating colonization. Imposing strong convection forces in the model resulted in a significant reduction of the bacteria from the intestine (not shown). Although we are not modeling the population level dynamics, release of *V. cholerae* from an infected host back into the environment as a consequence of diarrhea is an obvious assumption about how the disease is transmitted. Experimental evidence supports this assumption: in the infant rabbit, which models both colonization

Please cite this article as: Maria Spagnuolo, A., et al., A model for *Vibrio cholerae* colonization of the human intestine. J. Theor. Biol. (2011), doi:10.1016/j.jtbi.2011.08.028

of *V. cholerae* and diarrhea, intestinal bacterial counts increase steadily until the time secretory diarrhea is observed, when their numbers begin to plateau, suggesting that the diarrhea is causing shedding of intestinal bacteria (Ritchie et al., 2010).

While our preliminary work reveals many important aspects of the *V. cholerae* colonization process, many additional elements of the dynamics need to be explored. Among these are the interaction with diarrhea and the need to go from a 'local' simulation in one small region of the intestine to a larger scale simulation to see if 'global' behavior remains consistent over a much larger physiological scale. Finally, the ability to perform sensitivity analysis on the parameter space in the model is essential, and we are currently exploring that using methods developed in our group (Marino et al., 2008). To this end, we are developing a new numerical method in order to better study colonization dynamics. This new method will allow us to run simulations with more accurate results, since it will be a locally conservative method that handles jump discontinuities, such as those in the diffusion coefficient from the lumen to the mucus layer, accurately.

More specifically, we are interested in simulating the model with the same parameters as the baseline case, but with the following assumption on the growth rate: the bacteria in the lumen and mucus do not divide, but the bacteria that are adherent to the epithelium do divide. As it is now, the diffusion coefficients are too large for us to see a noticeable difference when we perform that simulation.

Our model is not limited to the study of *V. cholerae* colonization. It can be modified to study the dynamics of host–pathogen interactions with other microbes (Blakenship et al., 1991; McCrae and Stow, 1997). Significant efforts have been made in simulating bacterial motility in a viscous fluid (Childress and Peyret, 1976; Ghorai and Hill, 1999, 2000; Harashima et al., 1988; Hopkins and Fauci, 2002; Dillion and Fauci, 1995; Hill and Bees, 2002; Xue and Othmer, 2009; Cortez et al., 2004; Tival et al., 2005) as well as in simulating pattern formation and spatio-temporal complexity (Medvinsky et al., 2002) as well as in swimming cells (Kessler, 1986, 1989; Pedley and Kessler, 1987). More recent work on the bacterial motility in a fluid can be found in Bees and Hill (1998, 1999), Dillion and Fauci (1995), and Hopkins and Fauci (2002) and references therein. Our study is unique as the impact of the host environments on bacterial colonization are key the observed dynamics.

Acknowledgments

The authors thank Peter Shi for his contributions to earlier versions of the model and code. The authors would also like to thank Steve Wright for his discussions on the weak formulation of the model and Ethan Kubatko and Daniel J. Coffield Jr. for a discussion on the boundary condition. This work was supported by National Institute of Health (NIH) Grants R33HL092853, R01 HL106804 awarded to DEK and NIAID AI045125 awarded to V.J.D. This work was also supported by National Science Foundation (NSF) Grant OCI-749017 awarded to A.M.S.

Appendix A. Weak formulation of the bacterial density model

Let us multiply (12) by a smooth function w and integrate over Ω to obtain the following weak form (Ziemer, 1989) of the pde:

$$\int_\Omega \frac{\partial u}{\partial t} w\,dx - \int_\Omega w\,\mathrm{div}\{a\nabla u\}\,dx + \int_\Omega \mathrm{div}\{uv\} w\,dx + \int_\Omega k\alpha\,\mathrm{div}\{ue_r\} w\,dx - \int_\Omega cuw\,dx = \int_\Omega Sw\,dx.$$

which, after simplifying and applying the Divergence Theorem, becomes

$$\int_\Omega \frac{\partial u}{\partial t} w\,dx + \int_{\partial\Omega} (-a\nabla u + uv + k\alpha u e_r) w \cdot \mathbf{n}\,dS - \int_\Omega (-a\nabla u + uv + k\alpha u e_r)\cdot\nabla w\,dx - \int_\Omega cuw\,dx = \int_\Omega Sw\,dx$$

or

$$\int_\Omega \frac{\partial u}{\partial t} w\,dx + \int_{\partial\Omega_{in}\cup\partial\Omega_{out}} (-a\nabla u + uv + k\alpha u e_r) w \cdot \mathbf{n}\,dS + \int_{\partial\Omega_L} (-a\nabla u + uv + k\alpha u e_r) w \cdot \mathbf{n}\,dS - \int_\Omega (-a\nabla u + uv + k\alpha u e_r)\cdot\nabla w\,dx - \int_\Omega cuw\,dx = \int_\Omega Sw\,dx.$$

Since $e_r \cdot n = 0$ on $\partial\Omega_{in}$ and on $\partial\Omega_{out}$, it is clear that the above weak form becomes

$$\int_\Omega \frac{\partial u}{\partial t} w\,dx + \int_{\partial\Omega_{in}\cup\partial\Omega_{out}} (-a\nabla u + uv)\, w \cdot \mathbf{n}\,dS + \int_{\partial\Omega_L} (-a\nabla u + uv + k\alpha u e_r)\, w \cdot \mathbf{n}\,dS - \int_\Omega (-a\nabla u + uv + k\alpha u e_r)\ \cdot\nabla w\,dx - \int_\Omega cuw\,dx = \int_\Omega Sw\,dx.$$

Imposing the boundary conditions on $\partial\Omega_{in}\cup\partial\Omega_{out}$, the integral equation reduces to

$$\int_\Omega \frac{\partial u}{\partial t} w\,dx + \int_{\partial\Omega_{in}} w(-a\nabla u\cdot\mathbf{n} - uf(r))\,dS + \int_{\partial\Omega_L} (-a\nabla u + uv + k\alpha u e_r) w \cdot \mathbf{n}\,dS + \int_{\partial\Omega_{out}} w\left(-a\nabla u\cdot\mathbf{n} + u\left(-f(r) + \frac{L}{\pi R^2}\right)\right)dS - \int_\Omega (-a\nabla u + uv + k\alpha u e_r)\cdot\nabla w\,dx - \int_\Omega cuw\,dx = \int_\Omega Sw\,dx.$$

$$\int_\Omega \frac{\partial u}{\partial t} w\,dx - \int_{\partial\Omega_{in}} wuf(r)\,dS + \int_{\partial\Omega_L} (-a\nabla u + uv + k\alpha u e_r) w \cdot \mathbf{n}\,dS + \int_{\partial\Omega_{out}} wu\left(-f(r) + \frac{L}{\pi R^2}\right)dS - \int_\Omega (-a\nabla u + uv + k\alpha u e_r)\cdot\nabla w\,dx - \int_\Omega cuw\,dx = \int_\Omega Sw\,dx.$$

We impose the boundary conditions on $\partial\Omega_L$ to simplify the above equations to

$$\int_\Omega \frac{\partial u}{\partial t} w\,dx - \int_{\partial\Omega_{in}} wuf(r)\,dS + \int_{\partial\Omega_L} u\gamma(u) w \cdot \mathbf{n}\,dS + \int_{\partial\Omega_{out}} wu\left(-f(r) + \frac{L}{\pi R^2}\right)dS - \int_\Omega (-a\nabla u + uv + k\alpha u e_r)\cdot\nabla w\,dx - \int_\Omega cuw\,dx = \int_\Omega Sw\,dx.$$

Following Ladyzhenskaya (1969), let $J(\Omega)$ be the set of sufficiently smooth solenoidal vectors of compact support in Ω. Consider the following scalar product:

$$[v,\Phi] = \int_\Omega v_{x_k}\cdot\Phi_{x_k}\,dx$$

and the norm

$$\|v\| = \sqrt{[v,v]}.$$

Now, let $H(\Omega)$ be the complete Hilbert space defined as the completion of $J(\Omega)$ in the metric corresponding to this scalar product.

Define $V(\Omega)$ to be the closure in $(H^1(\Omega))^n$ of all smooth solenoidal vector fields. Then, the weak formulation of the problem is to:

Find all axially symmetric solutions $u \in H^1(\Omega \times J)$ and $v \in (L^2(\Omega,H^1(J)))^n \cap L^2(J,V(\Omega))$ such that

$$\int_{\Omega\times J} \frac{\partial v}{\partial t}\cdot \Phi \, dx\, dt - \mu \int_{\Omega\times J} \nabla v : \nabla \Phi \, dx\, dt = \int_{\Omega\times J} F\cdot \Phi \, dx\, dt,$$
$$\forall \Phi \in L^2(J; H(\Omega))$$

and

$$\int_{\Omega\times J} \frac{\partial u}{\partial t} w \, dx\, dt - \int_{\partial\Omega_{in}\times J} wuf(r)\, dS\, dt + \int_{\partial\Omega_L\times J} u\gamma(u) w\cdot \mathbf{n}\, dS\, dt$$
$$+ \int_{\partial\Omega_{out}\times J} wu\left(-f(r) + \frac{L}{\pi R^2}\right) dS\, dt - \int_{\Omega\times J} (-a\nabla u + uv + k\alpha u e_r)\cdot \nabla w \, dx\, dt$$
$$- \int_{\Omega\times J} cuw\, dx = \int_{\Omega\times J} Sw\, dx\, dt$$
$$\text{for all } w \in C^\infty(\overline{\Omega}\times J).$$

Note that the volumetric flow rate is conserved throughout Ω as can be seen by the following calculation:

$$0 = \int_\Omega \nabla\cdot v\, dx = \int_{\partial\Omega} v\cdot n\, dS$$
$$= \int_{\partial\Omega_{in}} -f(r)\, dS + \int_{\partial\Omega_{out}} \left(f(r) - \frac{L}{\pi R^2}\right) dS$$
$$+ \int_{\partial\Omega_L} v\cdot n\, dS.$$

If we now write $\Omega = \{(r,\theta,z) : 0 \le z \le Z, 0 \le \theta \le 2\pi, 0 \le r \le f(z)\}$, in cylindrical coordinates, and let $\tilde{\Omega} = \{(r,z) : 0 \le z \le Z, 0 \le r \le f(z)\}$, where $f(z)$ represents the epithelium boundary, then, converting to cylindrical coordinates and using the assumption of angular independence, the equations can be reduced to

$$2\pi \int_{\tilde{\Omega}} \frac{\partial u}{\partial t} wr\, dr\, dz - 2\pi \int_{\partial\tilde{\Omega}_{in}} wuf(r) r\, dS + 2\pi \int_{\partial\tilde{\Omega}_L} u\gamma(u) w\cdot \mathbf{n} r\, dS$$
$$+ 2\pi \int_{\partial\tilde{\Omega}_{out}} wu\left(-f(r) + \frac{L}{\pi R^2}\right) r\, dS$$
$$- 2\pi \int_{\tilde{\Omega}} (-a\nabla u + uv + k\alpha u e_r)\cdot \nabla w r\, dr\, dz$$
$$- 2\pi \int_{\tilde{\Omega}} cuwr\, dr\, dz = 2\pi \int_{\tilde{\Omega}} Swr\, dr\, dz.$$

References

Acheson, D.J., 1990. Elementary Fluid Dynamics. Oxford Applied Mathematics and Computing Science Series. Clarendon Press, Oxford.

Arnold, D.N., Brezzi, F., Cockburn, B., Marini, L.D., 2002. Unified analysis of discontinuous Galerkin methods for elliptic problems. SIAM J. Numer. Anal. 39 (5), 1749–1779.

Atsumi, T., Maekawa, Y., Yamada, T., Kawagishi, I., Imae, Y., Homma, M., 1996. J. Bacteriol. 178, 5024.

Bees, M.A., Hill, N.A., 1998. Linear bioconvection in a suspension of randomly swimming, gyrotactic micro-organisms. Phys. Fluids 10 (8), 1864–1881.

Bees, M.A., Hill, N.A., 1999. Non-linear bioconvection in a deep suspension of gyrotactic swimming micro-organisms. J. Math. Biol. 38 (2), 135–168.

Blakenship, C., et al., 1991. Colonization Control of Human Bacterial Enteropathogens in Poultry. Academic Press.

Blaser, M.J., Kirschner, D., Dynamics of Heliobacter pylori colonization in relation to the host response. Proc. Natl. Acad. Sci. USA 96, 8359–8364, Mathematics, Microbiology.

Blaser, M.J., Kirschner, D., 1995. The dynamics of *helicobacter pylori* infection of the human stomach. J. Theor. Biol. 176, 281–290.

Boin, M.A., Austin, M.J., Hase, C.C., 2004. Chemotaxis in *Vibrio cholerae*. FEMS Microbiol. Lett. 239 (1–8) PMID:15451094.

Butler, S.M., Camilli, A., 2004. Both chemotaxis and net motility greatly influence the infectivity of *Vibrio cholerae*. Proc. Natl. Acad. Sci. USA 101, 5018–5023 PMID:15037750.

Cash, R.A., Music, S.I., Libonati, J.P., Snyder, M.J., Wenzel, R.P., Hornick, R.B., 1974. Response of man to infection with *Vibrio cholerae*. I. Clinical, serologic, and bacteriologic responses to a known inoculum. J. Inf. Dis. 129, 45.

Childress, S., Peyret, R., 1976. A numerical study of two-dimensional convection by motile particles. J. Mec. 15 (5), 753–779.

Cockburn, B., Karniadakis, G.E., Shu, C.-W. (Eds.), 2000. Discontinuous Galerkin Methods. Theory, Computation and Applications. Lecture Notes in Computational Science and Engineering, vol. 11. Springer-Verlag, Berlin.

Cockburn, B., Shu, C.-W., 1998. The local discontinuous Galerkin method for convection–diffusion systems. SIAM J. Numer. Anal. 35, 2440–2463 MR 1655854 (99j:65163).

Cooper, S., 1997. Bacterial Growth and Division: Biochemistry and Regulation of Prokaryotic and Eukaryotic Division Cycles. Academic Press.

Cortez, R., Cowen, N., Dillon, R., Fauci, L., 2004. Simulation of swimming organisms: coupling internal mechanics with external fluid dynamics. Comput. Sci. Eng. 6 (3), 38–45.

Crank, J., 1975. Mathematics of Diffusion. Oxford University Press.

DiRita, V.J., 2000. Molecular basis of infection by *Vibrio cholerae*. In: Groisman, E. (Ed.), Principles of Bacterial PathogenesisAcademic Press, New York, pp. 457–508.

Dillion, R., Fauci, L., 1995. A microscale model of bacterial swimming, chemotaxis and substrate transport. J. Theor. Biol. 177, 325–340.

Douglas Jr., J., Huang, C.S., Spagnuolo, A.M., 2002. The approximation of nuclear contaminant transport in porous media. Comput. Appl. Math. 21 (2), 409–428.

Douglas Jr., J., Spagnuolo, A.M., 2001. The transport of nuclear contamination in fractured porous media. J. Korean Math. Soc. 38 (4), 723–761.

Douglas Jr., J., Spagnuolo, A.M., 2002. Parameter estimates for high-level nuclear transport in fractured porous media. Contemp. Math. 205, 173–183.

Foias, C., et al. (Eds.), 2001. Navier–Stokes Equations and Turbulence. Encyclopedia of Mathematics and its Applications, vol. 83. Cambridge University Press.

Freter, R., O'Brien, P.C., Macsai, M.S., 1981. Role of chemotaxis in the association of motile bacteria with intestinal mucosa: in vivo studies. Infect. Immun. 34, 234–240 PMID:7298185.

GNU Fortran (GFortran) project ⟨http://gcc.gnu.org/fortran/⟩.

Ghorai, S., Hill, N.A., 1999. Development and stability of gyrotactic plumes in bioconvection. J. Fluid Mech. 400, 1–31.

Ghorai, S., Hill, N.A., 2000. Wavelengths of gyrotactic plumes in bioconvection. Bull. Math. Biol. 62, 429–450.

Guentzel, M.N., Field, L.H., Eubanks, E.R., Berry, L.J., 1977. Use of fluorescent antibody in studies of immunity to cholerae in infant mice. Infect. Immun. 15, 539–548.

Happel, J., Brenner, H., 1987. Low Reynolds Number Hydrodynamics. Prentice-Hall, Englewood.

Harashima, A., Watanabe, M., Fujishiro, I., 1988. Evolution of bioconvection patterns in a culture of motile flagellates. Phys. Fluids 31 (4), 764–775.

Hill, N.A., Bees, M.A., 2002. Taylor dispersion of gyrotactic swimming microorganisms in a linear shear flow. Phys. Fluids 14, 2598–2605.

Hesthaven, J.S., Warburton, T., 2008. Nodal Discontinuous Galerkin Methods: Algorithms, Analysis, and Applications. Springer Texts in Applied Mathematics, vol. 54. Springer Verlag, New York.

Joseph, I.M., Kirschner, D., 2004. A model for the study of *Helicobacter pylori* interaction with human gastric acid secretion. J. Theor. Biol. 228, 55–80.

Hopkins, M., Fauci, L., 2002. A computational model of the collective fluid dynamics of motile microorganisms. J. Fluid Mech. 455, 149–174.

Kahn, M.U., Eeckels, R., Alam, A.N., Rahman, N., 1988. Cholera, rotavirus and ETEC diarrhea: some clinco=epidemiological features. Trans. R. Soc. Trop. Med. Hyg. 82, 485.

Kessler, J.O., 1986. Individual and collective dynamics of swimming cells. J. Fluid Mech. 173, 191–205.

Kessler, J.O., 1989. Path and pattern—the mutual dynamics of swimming cells and their environment. Comments Theor. Biol. 1 (2), 85–108.

Ladyzhenskaya, O.A., 1969. [1963], The Mathematical Theory of Viscous Incompressible Flow, Mathematics and its Applications, vol. 2 (Revised Second ed.), Gordon and Breach, New York, London, Paris, Montreux, Tokyo, Melbourne, pp. XVIII+224, MR0254401, Zbl 0184.52603.

Lee, S.H., Butler, S.M., Camilli, A., 2001. Selection for in vivo regulators of bacterial virulence. Proc. Natl. Acad. Sci. USA 98, 6889–6894 PMID:11391007.

Lee, S.H., Hava, D.L., Waldor, M.K., Camilli, A., 1999. Regulation of temporal expression patterns of *Vibrio cholerae* virulence genes during infection. Cell 99, 634–635.

McCrae, M.A., Stow, N.D., (Eds). 1997. Molecular aspects of host–pathogen interactions. In: Society for General Microbiology Symposium.

Marino, S., Hogue, I.B., Ray, C.J., Denise, K., 2008. A methodology for performing global uncertainty and sensitivity analysis. Syst. Biol. J. Theor. Biol. 254, 178–196 PMID:18572196.

Medvinsky, A.B., Petrovskii, S.V., Tikhonova, I.A., Malchow, H., Li, B.-L., 2002. Spatiotemporal complexity of plankton and fish dynamics. SIAM Rev. 44 (3), 311–370.

Pedley, T.J., Kessler, J.O., 1987. The orientation of spheroidal microorganisms swimming in a flow field. Proc. R. Sci. London B 231, 41–70.

Please cite this article as: Maria Spagnuolo, A., et al., A model for *Vibrio cholerae* colonization of the human intestine. J. Theor. Biol. (2011), doi:10.1016/j.jtbi.2011.08.028

Ritchie, J.M., Rui, H., Bronson, R.T., Waldor, M.K., 2010. Back tot he future: studying cholera pathogenesis using infant rabbits. MBio 1, e00047-10 (PMID: 20689747).

Rodo, X., Pascual, M., Fuchs, G., Faruque, A.S., 2002. ENSO and cholera: A nonstationary link related to climate change? Proc. Natl. Acad. Sci. USA 99, 12901–12906.

Rui, H., Ritchie, J.M., Bronson, R.T., Mekalanos, J.J., Zhang, Y., Waldor, M.K., 2010. Reactogenicity of live-attenuated *Vibrio cholerae* vaccines is dependent on flagellins. Proc. Natl. Acad. Sci. USA 107, 4359–4364 PMID:20160087.

Schrank, G.D., Verwey, W.F., 1976. Distribution of cholera organisms in experimental Vibrio cholerae infections: proposed mechanisms of pathogenesis and antibacterial immunity. Infect. Immun. 13, 195–203.

Shewchuk, J., 〈http://people.sc.fsu.edu/~jburkardt/c_src/triangle/triangle.html〉.

Shigematsu, M., Meno, Y., Misumi, H., Amako, K., 1995. The measurement of swimming velocity of *Vibrio cholerae* and *Pseudomonas aeruginosa* using the video tracking methods. Microbiol. Immunol. 39, 741.

Spira, W.M., Sack, R.B., 1982. Kinetics of early cholera infection in the removable intestinal tie-adult rabbit diarrhea model. Infect. Immun. 35, 952–957 (PMID:7068225).

Tival, I., Cisneros, L., Dombrowski, C., Wolgemuth, C.W., Kessler, J.O., Goldstein, R.E., 2005. Bacterial swimming and oxygen transport near contact lines. Proc. Natl. Acad. Sci. USA 102 (7), 2277–2282.

Wallace Hayes, A. (Ed.), Principles and Methods of Toxicology. Informa HealthCare USA, 2008, p. 1556.

Web site. 〈http://en.wikipedia.org/wiki/Small_intestine〉.

Web site. 〈http://chestofbooks.com/health/disease/Intestines/Structure-Of-The-Small-Intestine.html〉.

Xue, C., Othmer, H.G., 2009. Multiscale models of taxis-driven pattering in bacterial populations. SIAM J. Appl. Math. 70 (1), 133–169.

Ziemer, W.P., 1989. Weakly Differentiable Functions: Sobolev Spaces and Functions of Bounded Variation. Springer Verlag.

Please cite this article as: Maria Spagnuolo, A., et al., A model for *Vibrio cholerae* colonization of the human intestine. J. Theor. Biol. (2011), doi:10.1016/j.jtbi.2011.08.028